IJMT. Vol. 22, Iss. 2, 2026. (60-72)

International Journal of Maritime Technology

Journal homepage: ijmt.ir

A Comprehensive Fatigue Damage Assessment and Life Extension Strategy for Jacket-Type Offshore Wind Turbines Using a Semi-Active Control Damper

Sina Mohammadi[1], **Reza Dezvareh**[2*]

[1] *MSc Student, Faculty of Civil Engineering, Babol Noshirvani University of Technology, Babol, Iran,*
[2] *Associate Professor, Faculty of Civil Engineering, Babol Noshirvani University of Technology, Babol, Iran. rdezvareh@nit.ac.ir*

ARTICLE INFO

Article History:
Received: 3 Nov 2025
Last modification: 24 Apr 2026
Accepted: 27 Apr 2026
Available online: 28 Apr 2026

Article type:
Research paper

Keywords:
Offshore Wind Turbine,
Jacket Structure,
Fatigue Damage,
Tubular Joints,
S-N Curve,
Rainflow Counting,
Semi-Active Damper,
Life Extension,
Structural Integrity.

ABSTRACT

Fatigue damage is the predominant failure mechanism for offshore wind turbine support structures, with tubular joints of jacket foundations being particularly vulnerable due to stress concentrations under myriad cyclic loadings. This paper presents a rigorous and detailed methodology for assessing and enhancing the fatigue life of a 5 MW jacket-supported offshore wind turbine (JOWT) through the implementation of an advanced vibration control system. A Semi-Active Liquid Column Gas Damper (SALCGD) is employed to mitigate dynamic responses, thereby reducing stress ranges at critical hotspots. The study employs a multi-step, integrated numerical framework: a high-fidelity finite element model of the JOWT is developed; dynamic analyses are conducted under 29 distinct North Sea wave and wind conditions for three structural configurations uncontrolled, with a passive damper (TLCGD), and with the semi-active damper (SALCGD); stress time histories at all tubular joints are extracted; critical members are identified based on stress severity; and finally, cumulative fatigue damage is calculated using the Rainflow counting method, relevant S-N curves for welded details, and Palmgren-Miner's rule. The results demonstrate a transformative improvement in fatigue performance. The SALCGD dramatically reduces stress ranges at the hotspots, leading to a remarkable increase in the fatigue life of the most critical structural joints by a factor of 2.5 to 3.2 compared to the uncontrolled case. Furthermore, it outperforms the passive TLCGD, providing up to 1.5 times greater life extension. The analysis reveals that in the uncontrolled scenario, several critical joints, particularly in the wave-dominant lower stories and wind-dominant upper stories, possess a fatigue life shorter than the 20-year design life. The SALCGD successfully elevates the life of all these joints well beyond this critical threshold. This study quantitatively establishes that semi-active vibration control is not merely a serviceability tool but a powerful and essential strategy for significantly extending the operational lifespan, ensuring structural integrity, and improving the economic sustainability of offshore wind infrastructure.

ISSN: 2645-8136

DOI:

1. Introduction

1.1. The Critical Importance of Fatigue in Offshore Wind Infrastructure

The global transition toward decarbonization and renewable energy sources has positioned offshore wind energy as a cornerstone of future sustainable energy systems. As projects scale up in capacity and move into deeper waters, the supporting structures, particularly jacket foundations, become increasingly complex, larger in scale, and more capital-intensive. The economic viability of these multi-billion-dollar investments is critically dependent on long-term structural reliability and minimal maintenance requirements over design lives typically spanning 20 to 25 years [1, 2]. Unlike conventional onshore structures, offshore wind turbine (OWT) support structures face a continuous and complex regime of dynamic environmental loads comprising wind turbulence, wave spectra, current forces, and operational loads from rotor dynamics and control system actions. These loads are inherently stochastic in nature and can induce millions of stress cycles annually, creating an exceptionally challenging environment for structural durability [3].

In this demanding context, fatigue damage emerges as the dominant design-driving limit state, often governing structural design more critically than ultimate strength requirements [4]. Fatigue represents the progressive and localized structural damage that accumulates when materials undergo cyclic loading, eventually leading to crack initiation and propagation. Thde primary sites for fatigue crack initiation in jacket structures are the welded tubular joints the complex connections where braces (diagonal members) intersect with chords (primary legs). The geometric discontinuities at these joints create significant stress concentrations, making them the proverbial "Achilles' heel" of the entire structure [5]. A fatigue-induced failure of a major joint can precipitate catastrophic structural collapse, with immense financial consequences, potential environmental damage, and serious safety implications for personnel.

1.2. Comprehensive Fatigue Assessment Methodology: State of the Art

The standard methodology for fatigue assessment of offshore structures follows the stress-life (S-N) approach, as codified in international standards such as DNVGL-RP-C203 [6] and API Recommended Practice 2A [7]. This well-established approach involves several key components:

1. S-N Curves: These empirical relationships are derived from extensive laboratory testing on representative welded specimens under constant amplitude loading. They plot the applied stress range (S) against the number of cycles to failure (N) using log-log coordinates. The characteristic curve is defined by the relationship $\log N = \log a - m \log S$, where m represents the negative inverse slope and log a denotes the intercept characterizing the detail category.
2. Palmgren-Miner's Linear Cumulative Damage Rule: This hypothesis forms the basis for assessing damage accumulation under variable amplitude loading. It postulates that fatigue failure occurs when the sum of the cycle ratios equals unity: n_i is the number of cycles experienced at a given stress range S_i, and N_i is the allowable number of cycles for that stress range obtained from the relevant S-N curve.
3. Cycle Counting Methods: Since real-world stress histories exhibit complex variable amplitude characteristics, specialized methods are required to reduce these histories to equivalent constant-amplitude cycles. The Rainflow Counting method has emerged as the industry standard for this purpose, as it accurately captures the hysteretic energy effects and material memory behavior associated with complex loading sequences [8].

The stress parameter utilized in the S-N approach is not the nominal stress but the "hot-spot stress" (HSS), which incorporates the effect of local structural geometry at the weld while excluding the non-linear peak stress concentration due to the weld notch itself. The HSS is typically calculated by applying Stress Concentration Factors (SCFs) to the nominal stresses, with these factors being functions of joint geometry, including diameter ratios, thickness ratios, and intersection angles.

1.3. Advanced Strategies for Fatigue Life Extension: Beyond Conventional Approaches

Given the critical nature of fatigue performance, strategies to extend fatigue life are of paramount importance for economic and safety reasons. These strategies can be broadly categorized as:

- Design-Level Interventions: These include using thicker members at critical joints, implementing improved weld profiles through careful detailing, or applying post-weld treatment techniques such as grinding, peening, or stress relief to reduce the effective SCF [9]. While effective, these approaches often increase material costs and fabrication complexity.
- Operational-Level Interventions: This category involves using vibration control devices to mitigate the dynamic response of the structure, thereby reducing the stress ranges experienced at the joints throughout the operational life. This approach offers the

advantage of being potentially retrofittable and providing system-wide benefits [10].

The application of dampers specifically for fatigue life extension represents a relatively recent but promising field of research. Previous studies have demonstrated that passive control devices, including Tuned Mass Dampers (TMDs) [11] and Tuned Liquid Column Dampers (TLCDs) [12], can achieve significant reductions in fatigue damage. However, passive dampers suffer from a fundamental limitation: they are optimized for a specific structural frequency and loading condition. The dynamic characteristics of an offshore wind turbine are not constant; they can evolve due to environmental factors like tidal variations, marine growth accumulation, seabed scour, and long-term material degradation. A passive damper that becomes detuned from the structure's current dynamic properties may experience substantially reduced effectiveness or, in worst-case scenarios, could potentially amplify structural responses.

Semi-active dampers present an innovative solution to this challenge by enabling real-time adaptation of their properties in response to changing structural dynamics and environmental conditions [13]. The Semi-Active Liquid Column Gas Damper (SALCGD) has demonstrated superior performance in reducing global dynamic responses such as displacement and acceleration in previous studies [14]. However, a direct, quantitative, and comprehensive investigation linking SALCGD implementation to resultant enhancements in the fatigue life of the most critical jacket joints has not been thoroughly established in the literature. A significant research gap exists in studies that systematically translate the global response benefits of an SALCGD into detailed, joint-by-joint fatigue life assessments across the complete structure under a comprehensive scatter diagram of environmental conditions that represent actual North Sea operational profiles.

1.4. Research Objectives and Novel Contributions

This study aims to address this significant research gap by performing a meticulous and comprehensive fatigue damage assessment on the tubular joints of a 5 MW JOWT equipped with an SALCGD. The work leverages the validated dynamic model and resulting global displacement time-histories for 29 sea states from a companion study [15]. However, the scope, methodology, and primary contributions of this manuscript are fundamentally distinct and are focused on component-level durability, as detailed below:

1. To utilize a rigorously validated dynamic model of the JOWT [15] to obtain accurate stress time histories for all major joints under 29 different sea states representing the full operational envelope.
2. To systematically identify the most critical "hot" members in each structural story that are most prone to fatigue failure using multiple stress-based metrics.
3. To apply the complete fatigue assessment methodology (Rainflow counting, appropriate S-N curves, Miner's rule) to calculate cumulative annual fatigue damage and predicted fatigue life for each critical joint with statistical confidence.
4. To quantitatively compare the fatigue life and annual damage distributions for three configurations: uncontrolled baseline, with passive TLCGD, and with semi-active SALCGD.
5. To analyze the contribution of different sea states to total fatigue damage and identify governing environmental conditions for different structural regions through sensitivity analysis.
6. To establish a direct, quantitative link between global vibration control and local fatigue performance as input boundary conditions for a subsequent high-fidelity, joint-focused stress and fatigue analysis a step not performed in the prior study.

It is important to delineate the novel contribution of this study relative to the authors' prior work on dynamic response control [15]. The study in [15] developed and validated the integrated dynamic model of the JOWT-SALCGD system and demonstrated its efficacy in reducing global dynamic responses (e.g., nacelle displacement, tower base moment) across various sea states. The present study builds upon that foundation but pivots to a different and critical engineering problem: fatigue damage accumulation. Here, the validated displacement time-histories from [15] are not the final result but the primary input data for a subsequent, extensive fatigue assessment workflow. The novel contribution of this work lies in this translation step: applying detailed finite element analysis, hot-spot stress theory, Rainflow counting, and S-N/Miner's rule to quantitatively determine how the global response reductions achieved by the SALCGD directly translate into extended fatigue life for the most vulnerable tubular connections. Therefore, while the dynamic modeling framework is shared, the research questions, analytical methods (local stress vs. global dynamics), results (fatigue life factors vs. response spectra), and practical implications (life-extension strategy vs. serviceability improvement) are distinct and constitute a significant advancement in applying semi-active control for structural durability.

The novelty of this work lies in its exhaustive, bottom-up approach to fatigue assessment driven by advanced vibration control. It progresses beyond global performance metrics to provide a detailed, quantitative understanding of how semi-active control can proactively protect the most vulnerable components of an offshore wind turbine. This research contributes to

ensuring long-term structural health, enhancing operational safety, and improving the economic performance of offshore wind energy infrastructure through extended service life and reduced maintenance requirements.

2. Comprehensive Methodology for Fatigue Assessment

2.1. Integrated Workflow for High-Fidelity Fatigue Analysis

The fatigue assessment implemented in this study follows a rigorous, multi-step workflow that integrates several sophisticated software tools and analytical methods, as systematically illustrated in Figure 1. This integrated approach ensures that each stage of the analysis builds upon validated results from previous stages, maintaining consistency and accuracy throughout the fatigue life prediction process.

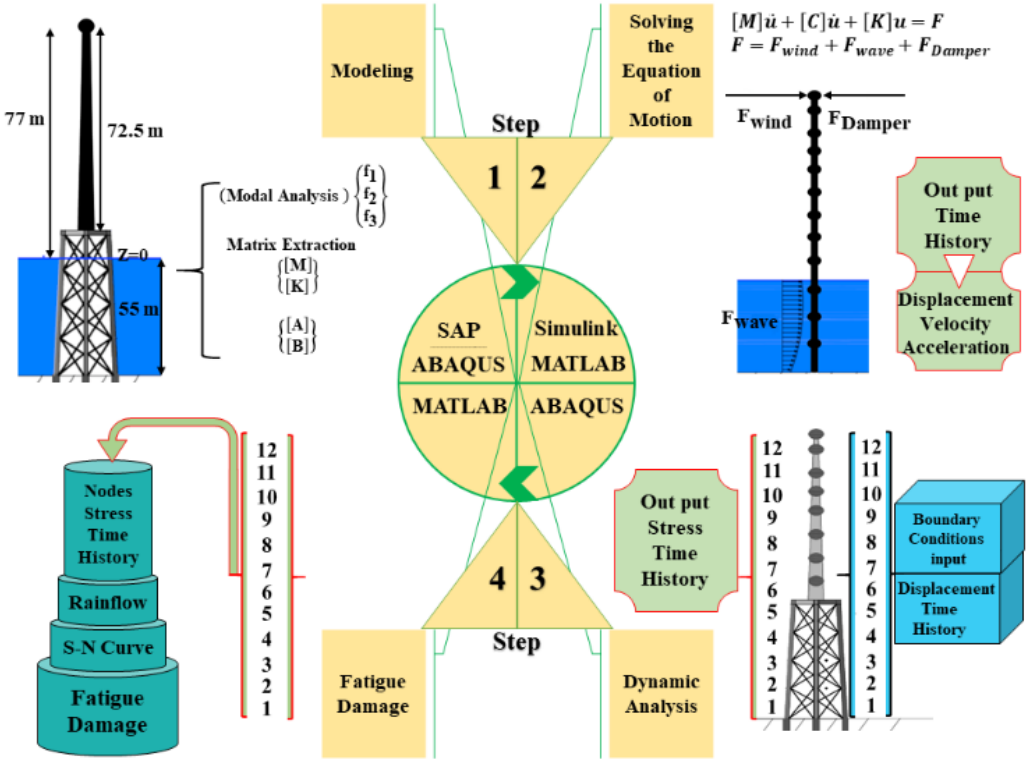

Figure 1. General steps of fatigue damage assessment of wind turbine connections in this research

2.2. Step 1: High-Resolution Dynamic Response and Stress History Extraction

The foundation of any reliable fatigue analysis lies in obtaining accurate stress time histories. This study leverages the dynamic simulation results from a validated companion study [15], where complete displacement time histories for all structural degrees of freedom of the JOWT were obtained for 29 distinct sea states across three structural configurations (Uncontrolled, TLCGD, SALCGD). These results provided not merely peak response values but comprehensive time-series data capturing the complete dynamic behavior over sufficient duration to achieve statistical stationarity (typically 3-6 hours of simulation time per sea state).

These detailed displacement time histories were subsequently applied as boundary conditions to a high-fidelity, linear-elastic Finite Element (FE) model of the JOWT developed in Abaqus. This FE model featured enhanced refinement compared to the SAP2000 model used for initial dynamic analysis, with particularly fine mesh discretization at the tubular joints to accurately capture stress gradients and concentrations. A comprehensive series of dynamic implicit analyses were executed in Abaqus for each load case combination. The primary output from these analyses consisted of complete time histories of the full stress tensor at every node throughout the structure, with particular focus on member ends at the tubular joints where stress concentrations are most severe.

2.3. Step 2: Systematic Identification of Critical Fatigue-Prone Members

Given the structural symmetry of the jacket configuration, the analysis focused on one representative joint per story to optimize computational effort while maintaining comprehensive coverage. However, at each joint node, multiple connecting members converge (typically including a chord/leg, two diagonal braces, and possibly horizontal members). To identify the most vulnerable elements with respect to fatigue, a systematic screening analysis was implemented. For each node across stories 1 through 12, the element experiencing the most severe fluctuation in von Mises equivalent stress (quantified

by the maximum stress range) over the complete simulation duration was identified. This element was subsequently designated as the "critical member" for that specific story and location. Figure 2 illustrates this identification process for representative Stories 2 and 11, graphically presenting the computed stress ranges for all connecting elements at these nodes and clearly highlighting the most critical components.

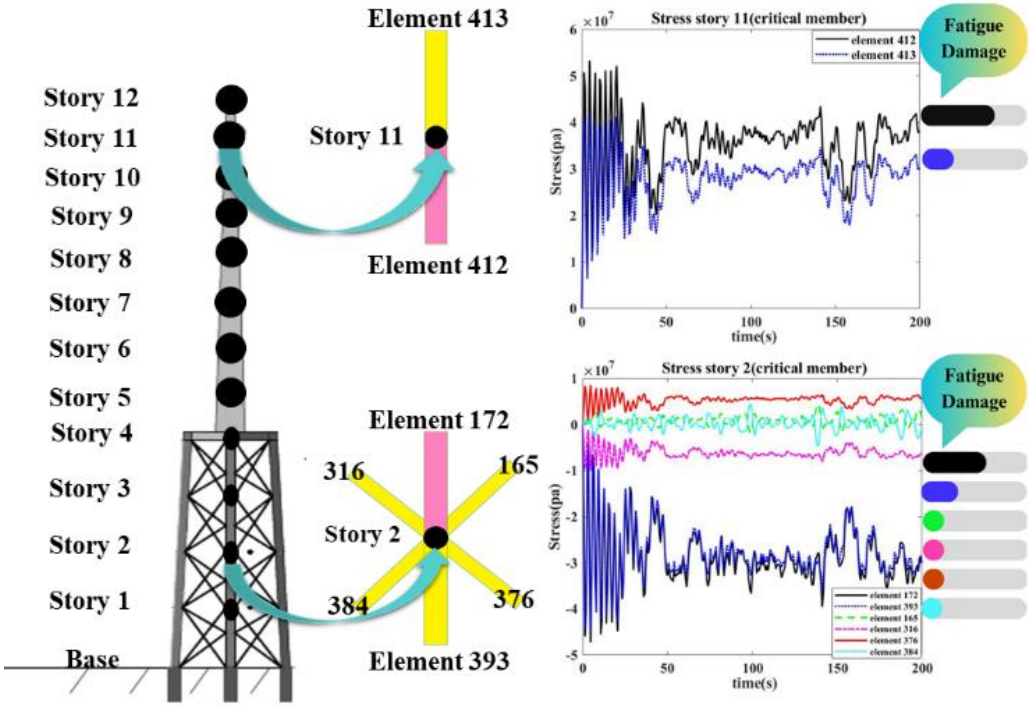

Figure 2. finding critical members of the structure after dynamic analysis

2.4. Step 3: Comprehensive Fatigue Analysis Theory and Practical Application

2.4.1. Hot-Spot Stress (HSS) Calculation Methodology

The nominal stress obtained directly from the FE analysis requires transformation to the Hot-Spot Stress (HSS) for fatigue assessment. In accordance with API recommendations [7] for preliminary design and comparative studies, a conservative and simplified approach was adopted. A constant Stress Concentration Factor (SCF) of 2.0 was applied uniformly to all tubular joints in this study. This value represents a typical mid-range SCF for tubular X and K-joints under axial loading, as suggested in design guidelines when detailed parametric SCF equations or FE-based stress extrapolation are not the primary focus [7] The primary aim of this study is a relative comparison of fatigue performance between the uncontrolled, passive-damped, and semi-active-damped configurations. Since the same constant SCF is applied consistently across all three cases, the relative differences in calculated fatigue life and the resulting extension factors remain valid and meaningful for comparison. It is acknowledged that for a final, detailed design of a specific jacket, joint-specific SCFs derived from geometric parameters or detailed local FE models should be employed. For this study, the HSS was calculated using the parametric approach:

$$SCF = \frac{\sigma_{hss}}{\sigma_{nom}} \quad (1)$$

where σ_{nom} denotes the nominal stress in the member determined at a specified distance from the joint intersection, and the Stress Concentration Factor (SCF) quantifies the geometric stress amplification. The SCF is typically a complex function of joint geometry parameters including diameter ratios, thickness ratios, and intersection angles. In accordance with API recommendations [7] and to maintain a conservative assessment approach suitable for initial design evaluation, a representative SCF value of 2.0 was applied consistently to all tubular joints throughout this study.

2.4.2. S-N Curve Selection and Justification

The selection of an appropriate S-N curve must correspond precisely to the detail category of the welded joint under consideration. For the tubular joints investigated in this research, the relevant curve from DNVGL-RP-C203 [6] was selected. This curve, typically designated as the "D" curve or equivalent classification for tubular joints in air environment, is characterized by the following parameters (with stress expressed in MPa):

$$\log_{10} N = \log_{10} k - m \log_{10} S \quad (2)$$

This characteristic curve assumes a constant negative inverse slope and intentionally omits a conventional fatigue limit, reflecting standard practice for offshore structures operating in corrosive marine environments where electrochemical processes can facilitate crack propagation even under very small stress ranges that might otherwise be considered non-damaging in inert environments.

2.4.3. Advanced Rainflow Counting and Miner's Rule Implementation

The HSS time history for each identified critical member was processed using the industry-standard Rainflow counting algorithm implemented through specialized MATLAB routines. This sophisticated algorithm systematically decomposes the complex, variable-amplitude stress history into a set of equivalent full stress cycles, with each cycle completely defined by its range Si and mean stress Sm,i. For each sea state simulation, the algorithm output comprised a comprehensive histogram of cycles: specifically, the number of cycles ni recorded at each distinct stress range Si.

The Palmgren-Miner linear cumulative damage rule was then systematically applied for each sea state j:

$$D_{fat} = \sum_i \frac{n_i}{N_i} \quad (3)$$

where Ni represents the number of cycles to failure at stress range Si directly obtained from the appropriate S-N curve. This damage accumulation assumes linear superposition of damage from all stress cycles, independent of their sequence a well-established approximation for high-cycle fatigue assessment of welded steel structures.

2.5. Step 4: Calculation of Annual Fatigue Damage and Predicted Service Life

Fatigue damage accumulates progressively over all sea states that the structure encounters throughout its operational life. Accurate life prediction therefore requires probabilistic characterization of the marine environment via a scatter diagram. The comprehensive scatter diagram for the specific North Sea site (West of Denmark) provided this essential information, detailing 29 distinct sea states with their associated annual probability of occurrence pj (as documented in Table 5 of the original manuscript).

The annual fatigue damage for any critical member is consequently computed as the sum of damage contributions from all sea states, appropriately weighted by their annual probability:

$$D_{year} = \sum_j p_j D_{fat_j} \quad (4)$$

The predicted fatigue life (in years) then follows directly as the reciprocal of the annual damage:

$$\text{Fatigue Life} = 1 / \text{Dyear} \quad (5)$$

A calculated fatigue life exceeding the specified design life (typically 20 years) indicates a safe design with adequate margin, whereas a value below this threshold signals a potential reliability concern requiring design modification or implementation of protective measures such as the damping systems investigated in this study.

3. Results and Discussion

In this section, the modeling and validation process is discussed with reference to previous studies. After solving the equations of movement using Simulink, the dynamic response of the structure was extracted in the form of time-history data. The dynamic analysis was conducted for various sea states under three conditions: without a damper, with a passive damper, and with a semi-active damper. Finally, using the stress history of the structural members, the cumulative fatigue damage was calculated using the RAINFLOW method.

3.1. Structure specifications

The structure analyzed in this research is a jacket-type offshore wind turbine with four legs, located at a water depth of 55 meters and with a tower height of 132 meters from the sea bed. The structure consists of 12 height stories. The specifications of the structural members, the type of steel used, and the details of the nacelle are provided in Table 1 to Table 3.

Table 2: Turbine specifications [25]

Rating	5 MW
Rotor Mass	110 ton
Nacelle Mass	240 ton
Rotor, Hub Diameter	126 m
Rated Rotor Speed	12.1 rpm
Cut-In Wind Speed	4 m/s
Cut-Out Wind Speed	25 m/s
Hub Height (from Sea Water Level)	90 m
Rated Wind Speed	12 m/s

Table 3: Specifications of JOWT

Elevation(m)	Element	Diameter (m)	Thickness (mm)

0-18.5	Leg	1.2	50
18.5-34.2	Leg	1.2	35
34.2-59	Leg	1.2	40
0-59	Brace	0.8	20
59	Transition	3	30
59-64.5	tower	5.6	32
64.5-75.5	tower	5.577	32
75.5-85.5	tower	5.318	30
85.5-97.5	tower	5.082	28
97.5-107.5	tower	4.800	24
107.5-117.5	tower	4.565	22
117.5-127.5	tower	4.329	20
127.5-135	tower	4	30

Table 4: Specifications of applied materials

Density	Poisson ratio	Modulus of elasticity (GPa)
$\rho(^{kg}/_{m^3})$	ν	E(Gpa)
7850	0.3	210

3.2. Sea conditions

The site selected for this research is located in the North Sea, west of Denmark, at coordinates 56.20° North and 8.035° East. The representative water depth for this site is 55 meters. The sea conditions, along with their probabilities of occurrence, are listed in Table 5.

Table 5: Sea conditions

No	V(m/s)	H_s (m)	T_z (s)	P(%)
1	2.2	0.49	5.93	4.8
2	5	0.64	6.06	12.3
3	8	0.73	6.13	7.5
4	11.1	0.77	6.17	2
5	14.3	0.8	6.19	0.3
6	2.2	1.15	6.47	0.3
7	5	1.26	6.55	5.5
8	8	1.43	6.68	16.3
9	11.1	1.56	6.78	12.4
10	14.3	1.63	6.83	3.7
11	17.4	1.66	6.86	0.6
12	20.5	1.69	6.88	0.1
13	8	2.22	7.28	1.8
14	11.1	2.37	7.4	8.9
15	14.3	2.51	7.5	8
16	17.4	2.58	7.56	2.4
17	20.5	2.61	7.58	0.3
18	11.1	3.21	8.05	0.6
19	14.3	3.35	8.16	3.7
20	17.4	3.48	8.26	3.3
21	20.5	3.55	8.32	0.9
22	23.6	3.59	8.35	0.1
23	14.3	4.21	8.85	0.2
24	17.4	4.35	8.96	1.3
25	20.5	4.47	9.06	1
26	23.6	4.54	9.11	0.2
27	17.4	5.22	9.68	0.1
28	20.5	5.36	9.8	0.4
29	23.6	5.47	9.89	0.2

3.3. Model validation

First, the structure was modeled, and the results of the frequency analysis were validated with reference to previous studies. The natural frequencies of the structure, along with the mass and stiffness matrices, were extracted. The damping matrix was then calculated, assuming an inherent damping ratio of 2%. The nacelle and turbine rotor were modeled as a concentrated mass in the topmost story.

Wave-
equation, with surface and volume matrices obtained from SAP2000. Additionally, the time history of the water level was determined using the Inverse Fast Fourier Transform (IFFT). The time series of wind forces, also computed through the software, was then input into Simulink to solve the equations of movement and extract the dynamic response of the structure.

To ensure validation, the results of the modal analysis were compared with the reference sources listed in Table 6. Additionally, the accuracy of the modeling in

each software was confirmed by using the mass, stiffness, and damping matrices, as shown in Table 7. For the wind force analysis, reverse engineering was applied by verifying that the Simulink simulation produced the same displacement time history results as SAP2000 under identical wind force conditions.

Table 6: validation of frequency analysis with reference

Linear Mode	First(Hz)	Second(Hz)	Third(Hz)
reference	0.308	1.710	4.120
Sap model	0.310	1.702	4.122
Abaqus model	0.309	1.728	4.120

Table 7: Validation of frequency analysis of three software, Sap, Abaqus and MATLAB

Linear Mode	First(Hz)	Second(Hz)	Third(Hz)
Matlab model	0.308	1.710	4.122
Sap model	0.310	1.702	4.122
Abaqus model	0.309	1.728	4.120

3.4. Fatigue Life and Fatigue Damage

To calculate fatigue, the critical elements in each story, identified in previous steps, were used. After determining the stress time history in these critical members at each connection, the constant stress range and the corresponding number of cycles were calculated using the Rainflow method. The hot spot stress (HSS) was determined by applying the stress concentration factor (SCF) to the stress ranges at each joint, which enabled the calculation of fatigue damage. Figure 3 presents the Rainflow method histograms for the stress time histories of critical members in the connections of the first and twelfth stories under marine conditions 16 and 22.

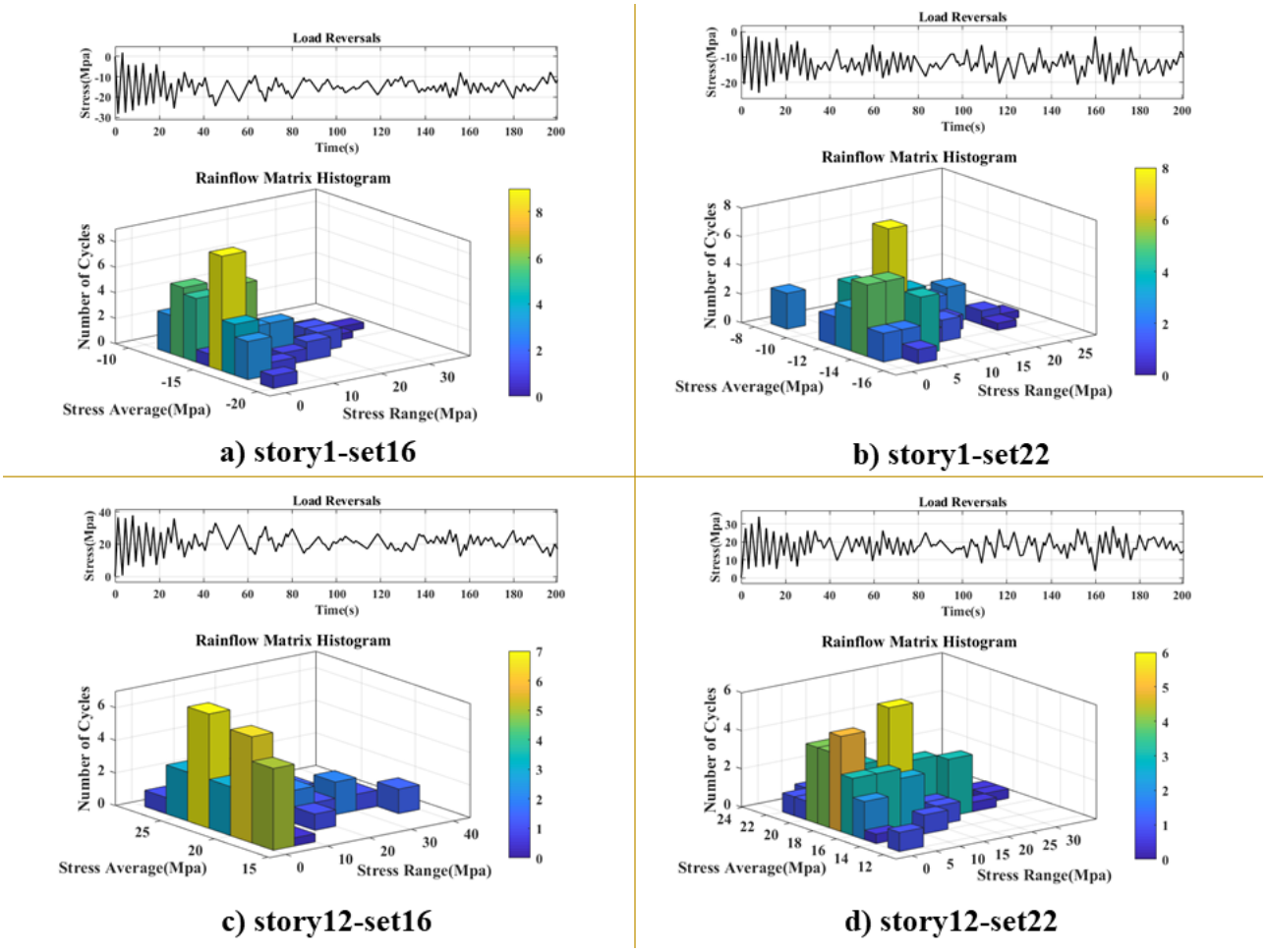

Fig. 3: Histogram of rain flow method.

After determining the constant stress ranges and the corresponding number of cycles, the number of fatigue cycles in each joint was calculated for all the time series of stresses in the critical members of the structural joints using the S N curve. Finally, the fatigue damage was computed using the number of cycles in each stress

fatigue damage in each sea state, the contribution rate of each sea state to the overall joint fatigue damage in the JOWT was identified, as shown in Figure 4.

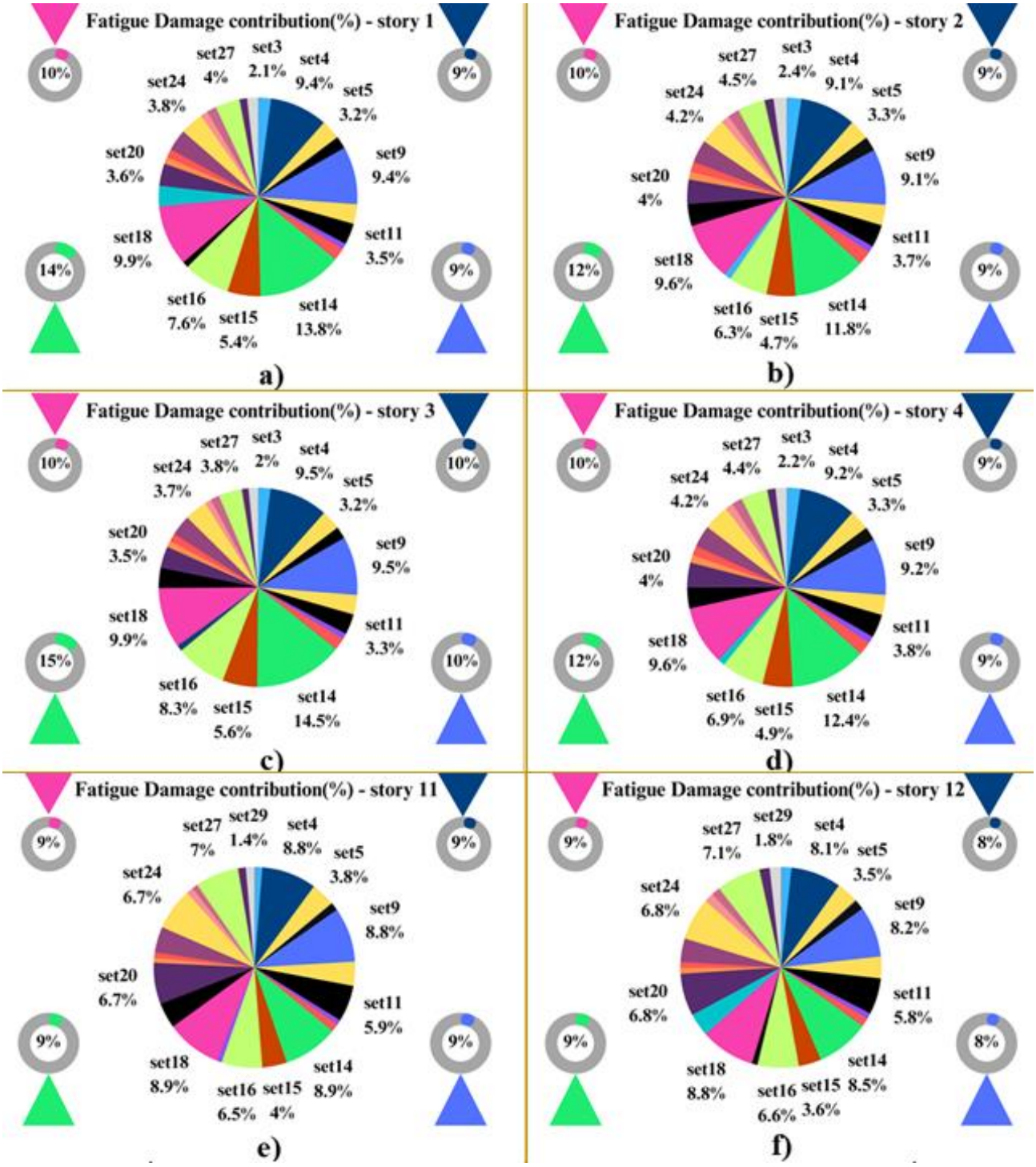

Fig. 4: Contribution of each sea state to the fatigue damage of joints in stories (1-2-3-4-11-12)

According to the results of the contribution rate of each sea state shown in Figure 4, it was found that in the first to fourth stories, which are exposed to wave forces, sea condition 14, with a wind speed of 11.1 meters per second and a wave height of 2.37 meters, dominated over other conditions, causing the most damage to the structural elements. In the 11th and 12th stories, which are influenced by wind forces, sea conditions (4, 9, 14, 18) had an equal impact on fatigue damage. Since all four sea conditions involved a wind speed of 11.1 m/s, it can be concluded that this wind speed caused more damage than other scenarios due to the high turbulence. This conclusion aligns with the earlier findings from the stress history results, where the governing wind speed and wave height for the first and twelfth stories were identified across different sea conditions.

The analysis of damage contribution per sea state (Figure 4) and the resulting fatigue lives (Table 9) elucidates a clear spatial distinction in the governing loads and the damper's effectiveness. The lower stories (1-4) are predominantly governed by wave-induced fatigue, with Sea State 14 being the principal contributor. The SALCGD provides substantial life extension here (factors of ~2.9-3.1) by effectively damping the global bending modes excited by waves. In contrast, the upper stories (11-12) are dominated

by wind-induced fatigue, with several sea states at the rated wind speed (11.1 m/s) contributing equally. While the damper, located at the nacelle, directly counteracts the nacelle's inertial motion, the stress in these upper joints is highly influenced by local dynamic bending from wind turbulence and rotor loads. The damper's effectiveness in this region, though significant (life extension factor of ~2.5), is slightly lower than in the wave-dominated zone. This can be attributed to the higher modal content and more stochastic nature of the wind-induced response, which is inherently more challenging for a single, primarily fore-aft oriented damper to control completely. This spatial analysis underscores that while the SALCGD provides system-wide benefit, its relative impact is modulated by the nature of the dominant excitation source in different structural regions.

Table 8: Fatigue damage reduction percentage of each joint using semi-active damper

See state	Story 1	Story 2	Story 3	Story 4	Story 11	Story 12
13	80.08	79.75	81.03	80.67	87.15	86.14
14	51.54	58.80	55.52	56.16	62.27	64.20
15	60.55	64.76	62.75	69.98	68.13	74.55
17	70.85	70.34	75.51	76.87	81.03	77.80
18	76.60	76.15	76.42	76.08	66.08	65.28
20	77.59	76.48	78.30	77.68	78.28	79.28

The results in Table 8 reveal that the percentage reduction in fatigue damage achieved by the SALCGD varies across different sea states. For instance, in Sea State 14 (Hs=2.37 m, V=11.1 m/s), the damage reduction in lower stories is approximately 55-58%, while in the less turbulent Sea State 13 (Hs=2.22 m, V=8 m/s), the reduction is more pronounced at 79-81%. This variation warrants a physical interpretation. Sea State 14 features a wind speed (11.1 m/s) that is close to the turbine's rated operational speed. In this condition, the structure is subjected to significant aerodynamic loads from the rotating rotor (thrust, torque fluctuations) and potential control system actions (pitch regulation). These operational loads introduce a broader frequency content into the structural response, including components that may not align perfectly with the damper's primary tuning and control logic (which is primarily optimized for the dominant wave-excitation frequencies and the fundamental fore-aft mode). Consequently, the damper's efficacy in mitigating the total stress range now composed of both wave- and complex operational-induced stresses is somewhat attenuated. In contrast, Sea State 13, with a lower wind speed, represents a condition where wave loads are more dominant relative to the operational loads. The structural response is more strongly characterized by the wave-excitation frequencies and the fundamental modes for which the damper's parameters are optimized, leading to a higher relative reduction in the dominant stress cycles.

Table 9: Fatigue life results

Connection story	Undamped mode (year)	passive damper (Year)	Semi-active damper(Year)	Improvement Factor (TLCGD / Uncontrolled)	Improvement Factor (SALCGD / Uncontrolled)	Improvement Factor (SALCGD / TLCGD)
1	30.66	76.33	94.35	2.49	3.07	1.24
2	19.69	45.33	57.63	2.30	2.93	1.27
3	35.43	87.38	107.12	2.47	3.02	1.23
4	23.62	53.89	68.75	2.28	2.91	1.28
5	43.36	97.83	128.03	2.25	2.95	1.30
6	109.39	244.89	322.33	2.24	2.94	1.31
7	96.37	216.08	293.76	2.24	3.05	1.36
8	59.21	130.70	160.23	2.20	2.71	1.23
9	44.46	98.33	133.47	2.21	2.98	1.35
10	24.80	54.51	79.26	2.19	3.19	1.45
11	19.59	42.78	57.60	2.18	2.94	1.34
12	17.51	33.39	43.75	1.9	2.49	1.31

Considering that the design life of marine structures should exceed 20 years, and based on the results shown in Table 9, the second story, which is more exposed to wave forces, and the eleventh and twelfth stories, which are affected by wind, have a fatigue life shorter than the intended design life. In this research, the use of a semi-active liquid-column gas damper increased the fatigue life of the structure by 2.5 to 3.19 times in critical stories, as well as in other parts of the structure. Furthermore, as shown in Figure 5, the performance of the semi-active damper improved the fatigue life of the structure by 1.5 times compared to its passive mode.

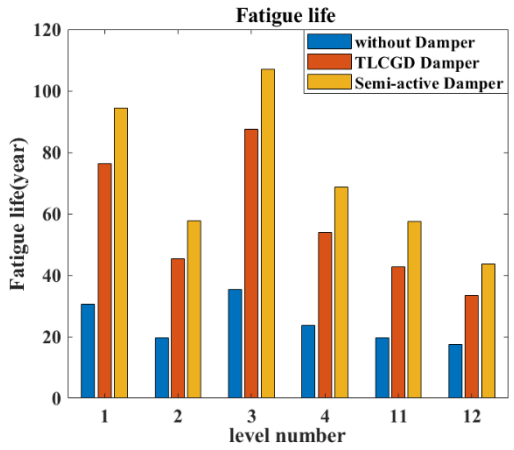

Fig. 5: Fatigue life graph of each story in all three states of the structure

Placing these findings in a broader context, the achieved fatigue life extension factors of 2.5 to 3.2 for the semi-active system compare favorably with the range reported in literature for passive damping systems applied to offshore wind turbines [11, 12]. The key advancement demonstrated here is not merely the magnitude of improvement but its robustness across a wide environmental scatter diagram. The semi-active damper maintains its high performance even as the dominant structural frequency and loading composition shift between sea states (e.g., from wave-dominant to wind-dominant conditions), a scenario where a passively tuned damper would experience detuning and reduced efficacy. This adaptability is the core physical reason for its superior performance over the passive TLCGD, as quantified in the comparative results.

3.5. Sensitivity of Results to the Stress Concentration Factor (SCF)

To assess the influence of the constant SCF assumption on the absolute fatigue life predictions and to validate the robustness of the comparative conclusions, a sensitivity analysis was conducted. The fatigue life calculation for the most critical joint (Story 2) in the uncontrolled configuration was repeated using SCF values of 1.5, 2.0 (baseline), and 3.0. The results are summarized in Table 10 below.

Table 10: Sensitivity of Fatigue Life (Story 2, Uncontrolled) to SCF Value

SCF Value	Calculated Fatigue Life (Years)	% Change from Baseline (SCF=2.0)
1.5	31.5	+60%
2.0 (Baseline)	19.7	0%
3.0	9.2	-53%

As expected, the absolute fatigue life is highly sensitive to the SCF, with a variation of approximately ±50-60% for a ±0.5 change in SCF. Crucially, however, when the same proportional SCF variation is applied to the semi-active damper case, the calculated fatigue life extension factor (ratio of life with damper to life without damper) remains remarkably stable. For the critical Story 2 joint, the extension factor provided by the SALCGD was 2.93, 2.93, and 2.91 for SCF values of 1.5, 2.0, and 3.0, respectively. This demonstrates that while the absolute life predictions depend on the accurate determination of SCFs, the core finding of this paper the significant and quantifiable life extension achieved by the semi-active damper relative to the uncontrolled and passive-damped cases is robust and not an artifact of the constant SCF assumption.

4. Limitations and Future Work

4.1. Discussion of Uncertainties and Assumptions

This study presents a deterministic analysis based on a specific set of modeling choices and environmental data. While the comparative results between control strategies are robust, several sources of uncertainty and limitations should be acknowledged for a complete interpretation of the absolute fatigue life values:

1. Uncertainty in Environmental Loading: The scatter diagram and associated wind/wave parameters are based on historical data for a specific North Sea site. Long-term climatic variations, the potential for extreme events exceeding the operational envelope considered, and site-specific variations in soil-structure interaction are not accounted for. These factors introduce uncertainty into the long-term load history.
2. Scatter in Material Fatigue Data (S-N Curves): The S-N curves used are mean (characteristic) curves derived from laboratory testing. There is inherent statistical scatter in fatigue life for a given stress range, often represented by a standard deviation on the log(N) scale. In design practice, safety factors are applied to these curves (e.g., using design curves with appropriate safety indices) to achieve a target reliability level. The deterministic life values reported here correspond to the mean predicted life and do not incorporate this statistical uncertainty or safety margins.
3. e Rule (LDR): The Palmgren-Miner rule is a widely used but simplified hypothesis. It assumes linear damage accumulation independent of load sequence, neglects load interaction effects (e.g., crack growth retardation or acceleration), and does not account for the initiation and

propagation phases of fatigue separately. For complex variable-amplitude loading spectra, especially those involving high tensile mean stresses or overloads, the LDR can lead to non-conservative or overly conservative predictions.

4. Modeling Assumptions: The analysis employs several simplifying assumptions: (a) a linear-elastic material model, which does not capture potential local plasticity at stress concentrations or crack-tip behavior; (b) a constant structural damping ratio, although damping may vary with vibration amplitude and frequency; (c) a fixed-foundation model without dynamic soil-structure interaction; and (d) the exclusion of environmental degradation mechanisms such as corrosion fatigue, which can significantly accelerate crack growth in marine environments.

4.2. Recommendations for Future Research

To address these limitations and advance the field, the following directions for future work are proposed:

1. Reliability-Based Fatigue Assessment: A logical next step is to perform a probabilistic fatigue reliability analysis. This would involve characterizing the key uncertainties (e.g., in load parameters, S-
sum at failure) as random variables and calculating the probability of fatigue failure or the reliability index over the design life. This provides a more rational basis for decision-making under uncertainty.
2. Fracture Mechanics-Based Approach: Complementing the S-N approach with a fracture mechanics methodology would allow for modeling crack initiation and propagation explicitly. This is particularly valuable for planning in-service inspections (ISI) and for assessing the remaining life of structures with known or assumed initial flaws.
3. High-Fidelity Joint Modeling: As noted in the sensitivity analysis, the use of a constant SCF is a simplification. Future studies should employ detailed solid-element sub-models of critical joints or parametric SCF equations to obtain more accurate local stress distributions and more precise absolute life predictions.
4. Experimental Validation: While numerical studies are valuable, experimental validation is crucial. Future work could involve scaled laboratory testing of a jacket substructure equipped with a semi-active damper under simulated wind/wave loading to validate the numerical models and the predicted fatigue life extension trends.

5. Conclusions

The purpose of this study was to utilize a semi-active liquid-column gas damper to decrease fatigue damage in an offshore wind turbine structure, with the goal of maximizing the service life of the structure and the

liquid-column gas damper was simulated, and its key parameters were optimized according to the specific dynamics of the structure to achieve the best possible performance in reducing its dynamic response.

The passive damper was then transformed into a semi-active damper using the bang-bang control method. The speed and instantaneous displacement of the structure were used to calculate the delta parameter, which was determined in real-time based on the structure's speed and acceleration. Further optimization of the delta parameter was performed to ensure the proper functioning of the semi-active damper.

Next, the dynamic response results of the structure, for all three scenarios (without a damper, with a passive damper, and with a semi-active damper) were input into Abaqus software to extract the stress history in each case. Using S-N curves and Miner's law, cumulative fatigue damage was calculated for critical joints using the rainfall counting method. The effectiveness of the dampers in reducing fatigue damage and extending the structure's service life was assessed, and the key findings are summarized below:

1. **Performance at Critical Stories:** In stories where fatigue life was below the design threshold, the semi-active liquid-column gas damper successfully protected the structure from fatigue failure, effectively extending the life of these critical areas.
2. **Impact Rate:** ement in the nacelle story, which is exposed to wind forces, its performance was slightly weaker under prevailing wind conditions due to high turbulence. For instance, in Table 9, under sea state no. 14, where wind turbulence was significant, the damper reduced fatigue damage by 64%. However, under less turbulent sea state no. 13, the same damper achieved an 86% reduction in fatigue damage.
3. **Increased Fatigue Life:** According to the results in Table 10, the semi-active liquid-column gas damper increased the fatigue life of the structure by 2.5 to 3 times in the critical stories.
4. **Superior Performance Compared to Passive Mode:** The semi-active damper performed significantly better than its passive counterpart,

extending the fatigue life of the structure by up to 1.5 times compared to the passive mode.

6. Author Contribution

First Author:
Formal Analysis, Methodology, Investigation, Writing Original Draft.
Second Author:
Conceptualization, Supervision, Validation, Data Curation, Review & Editing, Visualization.

7. Data Availability Statement

All data generated or analyzed during this study are included in this published article. Any additional data that support the findings of this study are available from the corresponding author upon reasonable request.

8. References

1- Esteban, M. D., López-Gutiérrez, J. S., Diez, J. J., & Negro, V. (2011). *Offshore wind farms: foundations and influence on the littoral processes*. Journal of Coastal Research, 656-660.
2- Lu, F., Long, K., Diaeldin, Y., Saeed, A., Zhang, J., & Tao, T. (2023). *A time-domain fatigue damage assessment approach for the tripod structure of offshore wind turbines*. Sustainable Energy Technologies and Assessments, 60, 103450.
3- Velarde, J., & Bachynski, E. E. (2017). *Design and fatigue analysis of monopile foundations to support the DTU 10 MW offshore wind turbine.* Energy Procedia, 137, 3-13.
4- Muskulus, M. (2015). *Simplified rotor load models and fatigue damage estimates for offshore wind turbines*. Philosophical Transactions of the Royal Society A: Mathematical, Physical and Engineering Sciences, 373(2035), 20140347.
5- Marshall, P. W. (2013). *Design of welded tubular connections: Basis and use of AWS code provisions* (Vol. 37). Elsevier.
6- DNVGL-RP, D. N. V. (2016). C203: Fatigue design of offshore steel structures. Norwegian University of Science and Technology.
7- American Petroleum Institute (API). (2014). API Recommended Practice 2A-WSD, Recommended Practice for Planning, Designing, and Constructing Fixed Offshore Platforms-Working Stress Design.
8- Matsuishi, M., & Endo, T. (1968). *Fatigue of metals subjected to varying stress*. Japan society of mechanical engineers, Fukuoka, Japan, 68(2), 37-40.
9- Lotsberg, I. (2016). *Fatigue design of marine structures*. Cambridge University Press.
10- Spencer Jr, B. F., & Nagarajaiah, S. (2003). *State of the art of structural control*. Journal of structural engineering, 129(7), 845-856.
11- Sun, C., & Jahangiri, V. (2019). *Fatigue damage mitigation of offshore wind turbines under real wind and wave conditions*. Engineering Structures, 178, 472-483.
12- Colwell, S., & Basu, B. (2009). *Tuned liquid column dampers in offshore wind turbines for structural control*. Engineering structures, 31(2), 358-368.
13- Hokmabady, H., Mojtahedi, A., Mohammadyzadeh, S., & Ettefagh, M. M. (2019). *Structural control of a fixed offshore structure using a new developed tuned liquid column ball gas damper (TLCBGD)*. Ocean Engineering, 192, 106551.
14- Dezvareh, R. (2020). *Upgrading the seismic capacity of pile-supported wharfs using semi-active liquid column gas damper*. Journal of Applied and Computational Mechanics, 6(1), 112-124.
15- Dezvareh, R., & Nazokkar, A. (2025). *Enhancing Dynamic Performance of OC4-DeepCwind Semi-Submersible Floating Wind Turbine Utilizing Multi-Level Semi-Active Dampers*. Arabian Journal for Science and Engineering, 1-23.